Inorganica Chimica Acta 374 (2011) 422–428

Contents lists available at ScienceDirect

Inorganica Chimica Acta

journal homepage: www.elsevier.com/locate/ica

Structures, spectroscopy and modeling of a rare set of isomeric copper(II) complexes

Peter Comba *, Shanthi Pandian, Hubert Wadepohl, Sebastian Wiesner

Universität Heidelberg, Anorganisch-Chemisches Institut, INF 270, D-69120 Heidelberg, Germany

ARTICLE INFO

Article history:
Available online 27 February 2011

Dedicated to Prof. W. Kaim

Keywords:
Distortional isomerism
Density functional theory
Ligand field
Diastereo isomer
Copper bispidine
Axial and rhombic

ABSTRACT

The structures and spectroscopic properties of various conformations of two diasteromeric pairs of enantiomers of pentacoordinate Cu^{II} bispidine complexes with chiral tetradentate ligands are reported. With one of the ligands an interesting type of distortional isomerism was observed experimentally, and this was studied in detail on the basis of the experimental structural and spectroscopic data (UV–Vis–NIR, EPR) and a DFT-, MM- and ligand-field-theory-based analysis.

1. Introduction

Cu^{II} bispidine complexes find a wide range of applications in biomimetic chemistry and catalysis (see Scheme 1 for the chiral tetradentate bispidines L discussed here) [1–7]. This is mainly due to the rigid 3,7-diazabicyclo[3.3.1]nonane (bispidine) backbone of the tetra-, penta- and hexadentate ligands, which enforces specifically distorted square pyramidal or *cis*-octahedral geometries, which are in particular highly complementary for the Jahn–Teller active Cu^{II} ions [8–12]. The shape and rigidity of the bispidine ligands leads to relatively flat potential energy surfaces (PES) with steep boundaries and various shallow minima in the flat area, i.e., a rigid ligand cavity and elastic coordination geometries [13,14]. This is of interest because the isomeric structures are close to degenerate and have significantly different structures and properties [5–7,11,15].

Bond-stretch or distortional isomers are molecules which differ only in the length of one or several bonds – much like conformers, they are species on a single potential energy surface with two or more minima, and there is a long and controversial history of distortional isomerism [16–20]. Complexes of the rigid bispidine ligands with flat PES and various nearly degenerate minima are potential candidates for distortional isomerism, and a number of examples have been discussed in detail.[1] This has interesting potential applications, since the near degenerate minima on the PES may have strikingly different structures and therefore may significantly differ in various molecular properties [22].

2. Results and discussion

The bispidine ligand L has two stereo centers when R ≠ H (carbon atoms 4 and 8 in Scheme 1), leading to two diastereomeric pairs of enantiomers of the corresponding pentacoordinate $[Cu^{II}(L)(Cl)]^+$ complexes. In each of the four configurations the methyl substituent at C8 may be axial (*ax*) or equatorial (*eq*), depending on the conformation of the corresponding six-membered chelate ring involving Npy1. The 4-(*R*)-8-(*R*)- and 4-(*R*)-8-(*S*) isomers of L^2 were isolated and their Cu^{II} complexes prepared and fully characterized (see Section 3). The synthesis of the ligands is based on a known method for the preparation of the chiral piperidone precursor [7,23], followed by a Mannich condensation with CH_2O and the corresponding amine fragment, i.e., optically pure (*R*)-α-Me- or (*R*)-α-Phe-picolylamine. Complexation to Cu^{II} was followed by chromatographic separation of the two diastereomeric forms.

The CD spectra of the pure diastereomers of the Cu^{II} complexes 4-(*R*)-8-(*R*)-$[(L^2)Cu^{II}(Cl)]^+$ and 4-(*R*)-8-(*S*)-$[(L^2)Cu^{II}(Cl)]^+$ (see Supplementary information) are, as expected, close to mirror images with positive Δε values in the CT and dd range of the spectra for 4-(*R*)-8-(*R*)-$[(L^2)Cu^{II}(Cl)]^+$ and negative values for 4-(*R*)-8-(*S*)-$[(L^2)Cu^{II}(Cl)]^+$ (see computed structures and their discussion, Fig. 1); the dd transitions for the former complex are at slightly lower energy than for the latter. This also emerges from the

* Corresponding author. Fax: +49 6221 546617.
E-mail address: peter.comba@aci.uni-heidelberg.de (P. Comba).

[1] Not all examples from the area of bispidine complexes published so far are bond-stretch isomers in a purist sense [2,9,12,13,21].

0020-1693/$ - see front matter © 2011 Elsevier B.V. All rights reserved.
doi:10.1016/j.ica.2011.02.047

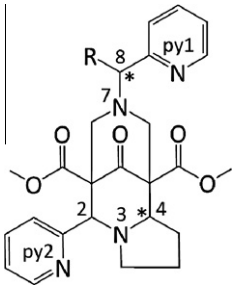

Scheme 1. Chemical structure of the chiral tetradentate bispidine ligands L; L^1: R = H, L^2: R = CH_3, L^3: R = C_6H_5.

solution electronic spectra (see Supplementary information for the spectra and below for the discussion of the transition energies). X-band EPR spectra of 4-(*R*)-8-(*R*)- and 4-(*R*)-8-(*S*)-$[(L^2)Cu^{II}(Cl)]^+$ (see Supplementary information) indicate that the Cu^{II} centers have axial symmetry with a d_{x2-y2} ground state. The spin Hamiltonian parameters are, as expected, slightly different for the two structures (see below).

Single crystal structural analyses of the ligands L^1, 4-(*R*)-8-(*R*)-L^2, 4-(*R*)-8-(*S*)-L^2, 4-(*R*)-8-(*R*)-L^3 and 4-(*R*)-8-(*S*)-L^3, as well as of the Cu^{II} complex of L^1, $[(L^1)Cu^{II}(Cl)]^+$ [7], and two conformers of the L^2-based Cu^{II} complex with axial and equatorial orientation of the 8-Me substituent, *ax*-4-(*R*)-8-(*S*)-$[(L^2)Cu^{II}(Cl)]^+$ and *eq*-4-(*R*)-8-(*S*)-$[(L^2)Cu^{II}(Cl)]^+$ are available (Fig. 1, Table 1; in all Cu^{II} structures, the ligands have, in contrast to the metal-free ligands and as usual [7], a hydrolyzed bridge-head keto group). All metal-free ligands have chair-boat conformations of the bispidine backbone with a well preorganized N3–py2 coordination pocket.

Interestingly, the unit cell of 4-(*R*)-8-(*S*)-$[(L^2)Cu(Cl)]^+$ includes two independent complex cations with strikingly different structures. The *eq*-4-(*R*)-8-(*S*)-$[(L^2)Cu(Cl)]^+$ complex, similar to that of the parent compound with the unsubstituted ligand L^1, has a distorted square pyramidal geometry (τ = 0.27 (L^2) versus 0.18 (L^1); τ = 0.0 for square pyramidal, 1.0 for trigonal bipyramidal [24]) and the pseudo-Jahn–Teller axis along the Cu–Npy2 bond. The apical Cu–Npy2 bond distance for *eq*-4-(*R*)-8-(*S*)-$[(L^2)Cu(Cl)]^+$ is 2.25 versus 1.98–2.10 Å for the other N-donor groups. The second structure, *ax*-4-(*R*)-8-(*S*)-$[(L^2)Cu(Cl)]^+$ has a geometry which is more distorted towards trigonal bipyramidal (τ = 0.34) and has a tertiary amine as the (pseudo)apical ligand (N3) with a Cu–N3 distance of 2.22 versus 2.10 Å. An ORTEP plot, based on the X-ray crystal structure analysis, of the two diastereomeric forms and of the parent L^1-based complex is shown in Fig. 1, the corresponding structural parameters are given in Table 1. Since these two isomers of 4-(*R*)-8-(*S*)-$[(L^2)Cu(Cl)]^+$ have very different geometries and appear in the same crystal lattice, they must be close to degenerate and therefore are typical examples for distortional isomerism.

For the L^2-based Cu^{II} complexes, the structural variation was therefore also studied with computational methods: the structures and relative stabilities of the four possible geometries (two conformations each [*ax* and *eq*] for the two diastereoisomeric forms of the coordinated ligand (4-(*R*)-8-(*S*)- and 4-(*R*)-8-(*R*)-(L^2)) as well as the electronic and spectroscopic properties and the energy barriers between the conformations were studied by density functional theory (DFT) as well as with empirical force field calculations with the ligand field molecular mechanics approach (LFMM) [12,25,26], and with ligand field theory (angular overlap model, AOM) calculations. The DFT- as well as the MM-optimized structures of the two conformers of the 4-(*R*)-8-(*S*)-(L^2)-based complexes are in very good agreement with the experimental structures (except for the Cu–Npy2 bond in the axial conformer, which is computed approx. 0.1 Å too long, see Table 1) and therefore allow predicting the two minimum structures of the 4-(*R*)-8-(*R*)-(L^2)-based complex, for which no experimental structural data are available. The DFT- and the MM-based computed Cu^{II} structures of this diastereomer are reasonably similar to each other, with the exception of the N7–Cu–Cl angle of the conformer with an equatorial 8-Me substituent, and this leads to some ambiguity with respect to the τ value and also to some deviation in the predicted Cu–Npy2 distance.

The generally observed accuracy of the structural data (X-ray versus DFT versus MM)[2] allows to make valid estimates of the relative stabilities of various isomers of $[(L^2)Cu(Cl)]^+$. Listed in Table 1 are the DFT-computed relative free energies and the MM-derived strain energy differences for all relevant structures.[3] The DFT-computed and LFMM-derived energy differences between *ax*- and *eq*-4-(*R*)-8-(*S*)-$[(L^2)Cu(Cl)]^+$ are 8.2 and 10.9 kJ/mol, respectively, in favor of the *ax* isomer, and those between *ax*- and *eq*-4-(*R*)-8-(*R*)-$[(L^2)Cu(Cl)]^+$ are 3.7 and 9.6 kJ/mol, with the *eq* isomer lower in energy.[4] It is interesting to note that similar energy differences were reported for the *axial* and *rhombic* structures of blue copper proteins, which exhibit a similar type of distortional isomerism [28].

A DFT-based relaxed PES scan for the 4-(*R*)-8-(*S*)-$[(L^2)Cu(Cl)]^+$ diastereoisomer was performed along various internal coordinates connecting the two conformers with *ax* versus *eq* 8-Me groups and elongations along Cu–N3 versus Cu–Npy2. Scans along the Cu–N3 and Cu–Npy2 modes alone did not interconvert the *ax* to *eq* geometries and *vice versa* but lead to distorted geometries with a 2.8 kJ/mol energy difference to the *eq*-4-(*R*)-8-(*S*)-$[(L^2)Cu(Cl)]^+$ minimum on the PES (11.0 kJ/mol to the *ax*-4-(*R*)-8-(*S*)-$[(L^2)Cu(Cl)]^+$ structure); the corresponding energies for the *eq*- and *ax*-4-(*R*)-8-(*R*)-$[(L^2)Cu(Cl)]^+$ isomers are 3.4 and 7.1 kJ/mol. Fig. 2 shows an overlay plot of the DFT-optimized structures of *ax*- and *eq*-4-(*R*)-8-(*S*)-$[(L^2)Cu(Cl)]^+$ together with the corresponding double-minimum PES and the computed transition structure.[5]

Angular overlap model (AOM) calculations (coordinates from the X-ray, DFT and MM derived structures) were used to compute the electronic dd transition energies and the g tensor parameters of all four isomers (see Table 2) [30–34]. The calculated g-values are in acceptable agreement with the simulated values except for g_{II} of *ax*-4-(*R*)-8-(*S*)-$[(L^2)Cu(Cl)]^+$.[6] The calculated dd transition energies indicate that the ligand field spectra of the four isomers are very similar, and this is what was observed experimentally (see Table 2 and Supplementary information). Clearly, the agreement between computed and observed transition energies is lower than one would hope (and lower than in other published examples [32,33], and this is partially due to deficiencies related to the computed structures but also due to the fact that ligand field parameters are not transferable [32]. However, the focus in this report is on the relatively small differences of the spectroscopic properties. Moreover, the small barrier

[2] The root mean square deviation (RMSD) between the DFT and X-ray structures is 0.07 Å for distances and 6.4° (*ax* isomer), 5.8° (*eq* isomer) for angles; the RMSD between the experimental and LFMM calculated structures is 0.07 Å for distances, 4.9° (*ax* isomer) and 2.4° (*eq* isomer) for angles.

[3] Note that no solvation corrections were adopted for the MM-derived relative energies; with crystal-structure-based force fields, averaged secondary interactions are believed to included [27].

[4] Note that DFT predicts *ax*-4-(R)-8-(S)-$[(L^2)Cu(Cl)]^+$ to be lowest in energy, while the absolute minimum structure predicted by MM is *eq*-4-(R)-8-(R)-$[(L^2)Cu(Cl)]^+$. This deviation may be due to the structural inaccuracies described above but this should not be overinterpreted because energy differences below 10 kJ/mol should be interpreted cautiously, specifically when very different methods have been used.

[5] Note that this obviously is not an optimized transition state structure but the indication is that there is a very low energy pathway for the structural interconversion; such a low activation barrier indicates that the distortional isomers may not easily be trapped and observed experimentally (e.g., not by X-band EPR spectroscopy; high-field (95 GHz) ESE-detected EPR was used to characterize the two electronic ground states of azurin mutants) [29].

[6] Model calculations indicate that this is not due to possible ligand exchange, i.e., the corresponding aqua complex leads to similar g-parameters.

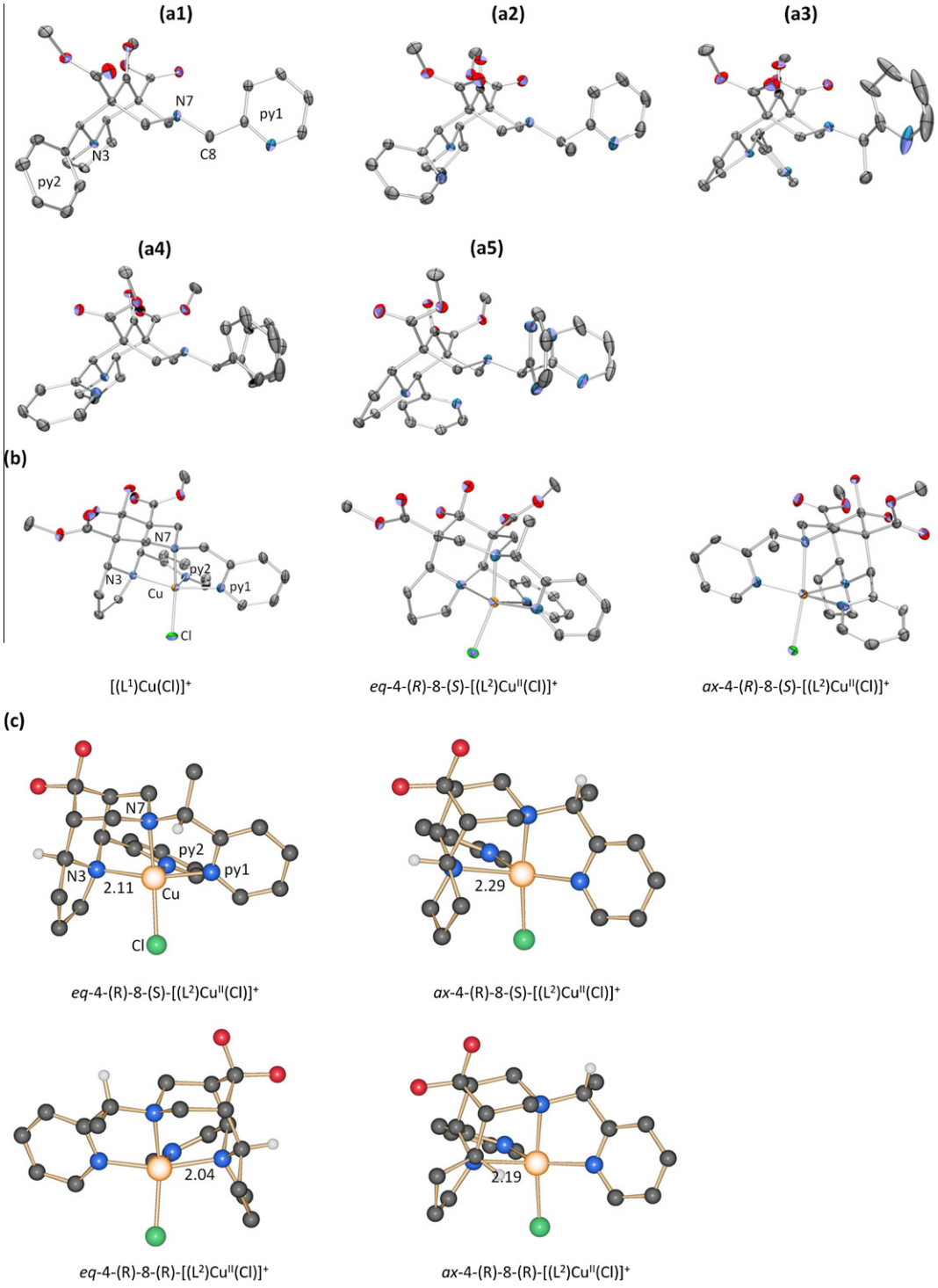

Fig. 1. Plots of the molecular structures of (a) X-ray structures of the ligands 1: L^1, 2: 4-(*R*)-8-(*R*)-L^2, 3: 4-(*R*)-8-(*S*)-L^2, 4: 4-(*R*)-8-(*R*)-L^3, 5: 4-(*R*)-8-(*S*)-L^3; (b) X-ray crystal structures of $[(L^1)Cu(Cl)]^+$ and of both conformers (*eq* and *ax*) of 4-(*R*)-8-(*S*)-$[(L^2)Cu(Cl)]^+$; and (c) DFT optimized structures of *eq*-4-(*R*)-8-(*S*)-$[(L^2)Cu^{II}(Cl)]^+$, *ax*-4-(*R*)-8-(*S*)-$[(L^2)Cu^{II}(Cl)]^+$, *eq*-4-(*R*)-8-(*R*)-$[(L^2)Cu^{II}(Cl)]^+$ and *ax*-4-(*R*)-8-(*R*)-$[(L^2)Cu^{II}(Cl)]^+$.

between the various isomers leads to fast dynamics, i.e., the observed spectra are obviously mixtures between different forms (see above).

In conclusion, the tetradentate chiral bispidine ligand L^2 with its two diastereoisomers leads to four isomeric pentacoordinate Cu^{II} complexes *eq*- and *ax*-4-(*R*)-8-(*S*)-$[(L^2)Cu(Cl)]^+$ and *eq*- and *ax*-4-(*R*)-8-(*R*)-$[(L^2)Cu(Cl)]^+$. Interestingly, there are striking differences in terms of the coordination geometries, and X-ray crystallography was used to show that *eq*-4-(*R*)-8-(*S*)-$[(L^2)Cu(Cl)]^+$ is best described as distorted square pyramidal, while the corresponding *ax*-isomer is distorted trigonal bipyramidal. The computed structures are in good agreement with experiment and allow to predicting a similar isomerism in the complexes with the 4-(*R*)-8-(*R*)-L^2-based complexes. This structural variation leads to subtle but small differences in the spectroscopic properties. However, the fact that the various isomers are close to degenerate and the shallow minima

Table 1
Comparison of experimentally determined, DFT (italics, in parentheses) and LFMM optimized (italics, in square brackets) structural parameters of the Cu^{II} complexes (distances in Å; angles in °; relative free energies in kJ/mol).

	$[(L^1)Cu(Cl)]^+$ [7]	*eq*-4-(*R*)-8-(*S*)-$[(L^2)Cu^{II}(Cl)]^+$	*ax*-4-(*R*)-8-(*S*)-$[(L^2)Cu^{II}(Cl)]^+$	*eq*-4-(*R*)-8-(*R*)-$[(L^2)Cu^{II}(Cl)]^+$	*ax*-4-(*R*)-8-(*R*)-$[(L^2)Cu^{II}(Cl)]^+$
Cu–N3	2.084(2)	2.099(4) *(2.11) [2.17]*	2.220(5) *(2.29) [2.24]*	*(2.04) [2.09]*	*(2.19) [2.19]*
Cu–N7	2.053(2)	2.036(5) *(2.09) [2.08]*	2.067(5) *(2.08) [2.08]*	*(2.18) [2.22]*	*(2.11) [2.11]*
Cu–Npy1	2.077(2)	1.983(5) *(2.03) [2.06]*	2.017(5) *(2.06) [2.09]*	*(1.99) [2.02]*	*(2.05) [2.09]*
Cu–Npy2	2.250(2)	2.259(5) *(2.35) [2.25]*	2.088(6) *(2.18) [2.19]*	*(2.27) [2.12]*	*(2.27) [2.18]*
Cu–Cl	2.280(2)	2.244(2) *(2.27) [2.25]*	2.269(2) *(2.26) [2.25]*	*(2.28) [2.24]*	*(2.26) [2.23]*
Npy1–Cu–N3	163.1(1)	161.7(2) *(165.3) [162.5]*	128.9(2) *(137.8) [134.4]*	*(167.9) [164.8]*	*(143.4) [134.4]*
Npy1–Cu–Npy2	93.015(1)	90.1(2) *(94.2) [93.1]*	150.8(2) *(144.9) [147.9]*	*(94.7)[93.8]*	*(137.8) [146.7]*
Npy2–Cu–N3	78.009(1)	77.8(2) *(77.0) [75.8]*	78.2(2) *(75.6) [75.9]*	*(78.6)[79.9]*	*(76.1) [77.1]*
N7–Cu–Cl	152.1(1)	145.4(2) *(153.7) [143.4]*	171.2(2) *(172.8) [166.6]*	*(136.5) [114.1]*	*(173.1) [170.0]*
τ	0.18	0.27 *(0.18) [0.25]*	0.34 *(0.47) [0.31]*	*(0.52) [0.83]*	*(0.50) [0.60]*
N3···N7	2.807(2)	2.832(2) *(2.92) [2.93]*	2.825(2) *(2.92) [2.92]*	*(2.96) [2.94]*	*(2.95) [2.91]*
Relative free energies		*(8.2) [19.7]*	*(0.0) [8.8]*	*(8.0) [0.0]*	*(11.7) [9.6]*

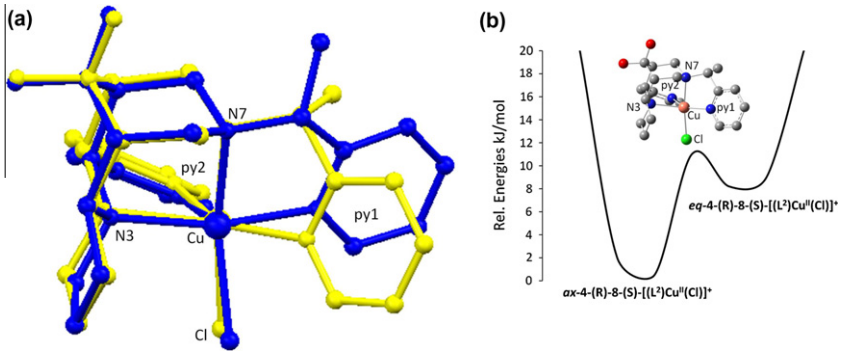

Fig. 2. (a) Overlay of *ax*-4-(*R*)-8-(*S*)-$[(L^2)Cu(Cl)]^+$ (light) and *eq*-4-(*R*)-8-(*S*)-$[(L^2)Cu(Cl)]^+$ (dark); and (b) PES of the interconversion of the two isomeric structures together with the distorted transition structure.

Table 2
Experimentally determined and calculated (AOM) transition energies and g-tensors for all four isomers, in comparison with the experimental data from *ax*-4-(*R*)-8-(*S*)-$[(L^2)Cu^{II}(Cl)]^+$ and *eq*-4-(*R*)-8-(*R*)-$[(L^2)Cu^{II}(Cl)]^+$.

Complex	Method	*E*(xy) (cm^{-1})	*E*(yz) (cm^{-1})	*E*(xz) (cm^{-1})	*E*(z^2) (cm^{-1})	g_1	g_2	g_3
ax-4-(*R*)-8-(*S*)-$[(L^2)Cu^{II}(Cl)]^+$	X-ray	15 680	13 200	14 230	8560	2.04	2.07	2.23
	DFT-AOM	14 510	12 380	13 340	8780	2.04	2.09	2.24
	MM-AOM	14 220	12 100	12 870	8010	2.04	2.09	2.25
eq-4-(*R*)-8-(*S*)-$[(L^2)Cu^{II}(Cl)]^+$	X-ray	14 290	10 710	12 410	5420	2.06	2.06	2.25
	DFT-AOM	14 790	12 950	13 800	10 240	2.04	2.07	2.23
	MM-AOM	13 220	10 330	11 990	7760	2.05	2.08	2.26
ax-4-(*R*)-8-(*R*)-$[(L^2)Cu^{II}(Cl)]^+$	DFT-AOM	14 270	12 300	13 300	8590	2.04	2.09	2.24
	MM-AOM	14 150	12 080	12 910	7560	2.03	2.10	2.25
eq-4-(*R*)-8-(*R*)-$[(L^2)Cu^{II}(Cl)]^+$	DFT-AOM	14 850	12 330	13 570	9590	2.01	2.11	2.21
	MM-AOM	14 030	11 310	12 500	7630	2.02	2.10	2.24
ax-4-(*R*)-8-(*S*)-$[(L^2)Cu^{II}(Cl)]^+$	exp	15 600		14 700	10 500	2.05	2.05	2.35
eq-4-(*R*)-8-(*R*)-$[(L^2)Cu^{II}(Cl)]^+$	exp	16 600		13 600	10 500	2.06	2.06	2.25

on the potential energy surfaces are connected with low energy barriers, leads to fast dynamics and prevents to trap and spectroscopically characterize the various structures.

3. Experimental

3.1. General

Chemicals (Aldrich, Fluka) and solvents were of highest possible grade and used as purchased. Elemental analyses were performed by the analytical laboratories of the chemical institutes of the University of Heidelberg.

Electronic spectra were measured with a Tidas II J&M or a Jasco V-570 UV–Vis–NIR-spectrophotometer. *EPR* (*X-band*, 9.5 GHz) *spectra* at liquid N_2 temperature were recorded on a Bruker Biospin ELXSYS E500 spectrometer with a rectangular TE_{102} cavity mode. The spin Hamiltonian parameters were obtained by simulation with X-Sophe [35]. *NMR spectra* were recorded at 200.13 MHz (^1H) and 50.33 MHz (^{13}C) on a Bruker AS-200 or a Bruker DRX-200 instrument with the solvent signals used as reference. *IR spectra* were recorded with a Perkin–Elmer Spectrum 100 FT-IR spectrometer instrument from KBr pellets. *Mass spectra* were obtained with a JEOL JMS-700 or Finnigan TSQ 700/Bruker ApexQe hybrid 9.4 FT-ICR instrument. For *optical rotations* a Jasco DIP 370 polarimeter and for *CD spectra* a Jasco J 710 spectropolarimeter were used.

3.2. Syntheses

3.2.1. Piperidone precursor pL (6,8-dimethyl-7-oxo-5-(pyridinyl-2yl)octahydroindolizin-6,8-dicarboxylate)

γ-Aminobutyraldehydediethylacetal (18.4 g, 11.4 mmol) was heated (65 °C) in HCl (1.5 M in MeOH, 200 ml). At ambient temper-

ature, pyridin-2-aldehyd (12.2 g, 11.4 mmol) and acetondicarboxylate–dimethylester (19.8 g, 11.4 mmol) were added and the pH was adjusted to 4 by Na_2CO_3. After stirring at ambient conditions for 1 week, the pH was adjusted to 9 (Na_2CO_3), and the solution was extracted with CH_2Cl_2 (five times). The combined CH_2Cl_2 fraction was dried over $MgSO_4$ and evaporated to dryness. The oily residue was washed with diethylether and dissolved in MeOH (80 ml); H_2O (10 ml) was added under stirring. At 4 °C, a white solid crystallized and was removed by filtration, washed with EtOH/H_2O 1:1 and dried in vacuum. Yield: 3.3 g (1 mmol; 9%), white solid. *Anal.* Calc. for $C_{17}H_{20}N_2O_5$: C, 61.44; H, 6.07; N, 8.43. Found: C, 61.37; H, 6.04; N, 8.42%. ^{1}H NMR (200 MHz, $CDCl_3$): δ = 1.94 (m, 3H, CH–C*H*$_2$–C*H*$_2$); 2.30 (m, 2H, N–C*H*$_2$–C*H*$_2$); 2.81 (td, ^3J = 2.72 Hz, ^3J = 8.6 Hz, 1H, N–C*H*–CH$_2$); 3.18 (m, 1H, N–C*H*$_2$–CH$_2$); 3.74 (s, 3H, O–C*H*$_3$); 3.86 (d, ^3J = 11.2 Hz, 1H, CO–C*H*–CO); 3.97 (s, 3H, O–C*H*$_3$); 4.19 (d, ^3J = 10.7 Hz, 1H, CO–C*H*–CO); 4.50 (d, ^3J = 11.04 Hz, 1H, N–C*H*–Py); 7.45 (m, 2H, H_{Ar}); 7.86 (td, ^3J = 7.6 Hz, ^4J = 1.77 Hz, 1H, H_{Ar}); 8.86 (d, ^3J = 5.53 Hz, 1H, H_{Ar}). ^{13}C NMR (50 MHz, $CDCl_3$): δ = 21.75 (1C, N–CH$_2$–*C*H$_2^-$); 30.15 (1C, CH–*C*H$_2$–CH$_2^-$); 51.13 (1C, N–*C*H$_2$–CH$_2^-$); 52.41 (1C, O–*C*H$_3$); 52.54 (1C, O–*C*H$_3$); 61.51 (1C, CO–*C*H–CO); 62.68 (1C, N–*C*H–Py); 67.10 (1C, CO–*C*H–CO); 69.10 (1C, N–*C*H–CH$_2$); 123.67, 124.53, 137.09, 150.63, 157.67 (5C, *C*-arom.); 170.5 (1C, *C*OOCH$_3$); 171.80 (1C, *C*OOCH$_3$); 199.82 (1C, *C*=O). MS: FAB $C_{17}H_{20}N_2O_5$, $[M+H]^+$ = 333.1.

3.2.2. L^1 (9-Oxo-2-(pyridin2-yl)-7-(pyridin-2yl-methyl)-3,7-diazatricyclo[3.3.3^{3,4}.1]dodecan-1,5-dicarbonsäuredimethylester)

7-Oxo-5-(pyridinyl-2yl)octahydroindolizine-6,8-dicarboxylate-dimethylester (4.6 g, 13.8 mmol) were suspended in EtOH (35 ml) and cooled to 0 °C. 2-Aminomethylpyridin (1.6 g, 14.7 mmol) were added dropwise, and the solution was left stirring for 30 min before formaldehyde (2.7 ml, 32.4 mmol, 37% in H_2O) was added. After 24 h stirring at ambient temperature, the solution was evaporated to dryness in vacuum, dissolved in (CH_2Cl_2, 50 ml) and dried over $MgSO_4$. This solution was evaporated to dryness and the residue was recrystallized from EtOH/Et_2O. Yield: 2.8 g (6.0 mmol, 43.5%), white solid. X-ray structure of the racemic ligand (co_SEW 4a). *Anal.* Calc. for $C_{25}H_{28}N_4O_5$: C, 64.64; H, 6.08; N, 12.06. Found: C, 64.22; H, 6.08; N, 11.89%. ^{1}H NMR (200 MHz, $CDCl_3$): δ = 1.70–2.35 (m, 4H, CH–C*H*$_2$–C*H*$_2$); 3.18 (td, ^2J = 15.2 Hz, ^3J = 8.4 Hz, 2H, N–C*H*$_2$); 3.60–3.85 (m, 3H); 3.88 (s, 3H, OC*H*$_3$); 3.97 (s, 3H, OC*H*$_3$); 4.04 (s, 2H, Py–C*H*$_2$); 4.36 (s, 1H, Py–C*H*–N); 7.25–7.90 (m, 6H, H_{Ar}); 8.69 (d, ^3J = 4.8 Hz, H_{Ar}); 8.74 (d, ^3J = 4.8 Hz, H_{Ar}). ^{13}C NMR (50 MHz, $CDCl_3$): δ = 21.37 (1C, N–CH$_2$–*C*H$_2^-$); 25.86 (1C, CH–*C*H$_2$–CH$_2^-$); 50.47 (1C, N–*C*H$_2$–CH$_2^-$); 52.41, 52.24 (2C, O–*C*H$_3$); 55.24, 56.00 (2C, N–*C*H–C$_q$); 62.43, 63.06 (2C, *C*$_q$); 62.74 (1C, N–C*H*$_2$–Py); 121.90, 122.74, 122.91, 124.61, 136.03, 136.27, 148.62, 149.25, 156.70, 158.72 (10C, *C*$_{Ar}$); 169.55, 170.00 (2C, –O*C*H$_3$); 202.59 (1C, C=O). MS: FAB $C_{25}H_{28}N_4O_5$ $[M+H]^+$ = 465.2.

3.2.3. L^2 (R,rac)-9-oxo-2-(pyridin2-yl)-7-(1-(pyridin-2yl)-ethyl)-3,7-diazatricyclo[3.3.3^{3,4}.1]dodecan-1,5-dicarbonsäuredimethylester

7-Oxo-5-(pyridinyl-2yl)octahydroindolizin-6,8-dicarboxylate-dimethylester (2.5 g, 7.5 mmol), suspended in MeOH (60 ml) was cooled to 0 °C. (*R*)-1-(pyridinyl-2yl)ethylamine (0.92 g, 7.5 mmol) was added dropwise and stirred for 30 min. Formaldehyde (1.8 ml, 15 mmol, 37% in H_2O) was added and, after stirring at ambient temperature for 24 h, the solution was evaporated to dryness in vacuum, dissolved with the minimum amount of CH_2Cl_2 and dried over $MgSO_4$. The solution was evaporated to dryness and the residue crystallized from EtOH/Et_2O. Yield: 1.8 g (3.7 mmol, 50%), white solid (1:1 mixture of [R,S], [R,R] diastereomers). X-ray structure (co_SEW 17a). *Anal.* Calc. for $C_{26}H_{30}N_4O_5$: C, 65.26; H, 6.32; N, 11.71. Found: C, 65.28; H, 6.35; N, 11.68%. ^{1}H NMR (400 MHz, $CDCl_3$): δ = 1.47 (t, ^3J = 6.7 Hz, 6H, CH–C*H*$_3$); 1.55–2.15 (m, 10H, C*H*$_2$); 2.91 (q, ^3J = 8.2 Hz, 2H); 3.10 (m, 2H); 3.43 (t, ^3J = 10.9 Hz, 2H); 3.59 (dd, ^4J = 2.7 Hz, ^3J = 11.0 Hz, 2H); 3.69 (s, 3H, –OC*H*$_3$); 3.71 (s, 3H, –OC*H*$_3$); 3.75 (s, 3H, –OC*H*$_3$); 3.78 (s, 3H, –OC*H*$_3$); 4.04 (d, ^3J = 11.5 Hz, 2H); 4.10 (d, ^3J = 11.7 Hz, 2H); 4.19 (d, ^3J = 4.1 Hz, 2H); 7.15–7.70 (m, 12H, H_{Ar}); 8.50–8.60 (m, 4H, H_{Ar}). ^{13}C NMR (50 MHz, $CDCl_3$): δ = 17.42, 17.50, 21.37, 25.90, 30.90, 50.50, 50.57, 51.15, 51.79, 52.22, 52.30, 52.34, 52.45, 53.78, 54.46, 62.52, 62.68, 63.19, 64.77, 64.82, 68.63, 68.78, 72.01, 72.05, 121.90, 121.94, 122.34, 122.50, 122.93, 122.97, 124.59, 124.68, 136.04, 136.11, 136.22, 148.35, 149.32, 149.34, 156.81, 156.83, 163.47, 163.50, 169.67, 169.88, 170.20, 170.26, 202.59, 202.63, 206.92. MS: FAB $C_{26}H_{30}N_4O_5$ $[M+H]^+$ = 479.3. $[\alpha]^D_{20}$ = 36.3° (R, rac) (c = 1 in $CHCl_3$).

3.2.4. L^3 (S,rac)-9-Oxo-2-(pyridin2-yl)-7-(phenyl(pyridin-2yl)-methyl)-3,7-diazatricyclo[3.3.3^{3,4}.1]-dodecan-1,5-dicarbonsäuredimethylester

7-Oxo-5-(pyridinyl-2yl)octahydroindolizine-6,8-dicarboxylate-dimethylester (900 mg, 2.7 mmol), suspended in EtOH (10 ml) was cooled to 0 °C. (S)-phenyl(pyridin-2-yl)methylamine (500 mg, 2.7 mmol) were added dropwise, stirred for 30 min and formaldehyde (0.5 ml, 6 mmol, 37% in H_2O) were added. After 24 h at ambient temperature, the solvent was removed in vacuum, the residue dissolved in little CH_2Cl_2 and dried over $MgSO_4$. The solution was evaporated to dryness and the residue crystallized from EtOH/Et_2O. Yield: 660 mg (1.2 mmol, 32%), white solid (1:1 mixture of [S,S], [S,R] diastereomers). X-ray structure (co_SEW 20). *Anal.* Calc. for $C_{31}H_{32}N_4O_5$: C, 65.87; H, 5.97; N, 10.36. Found: C, 65.32; H, 6.00; N, 10.14%. ^{1}H NMR (200 MHz, $CDCl_3$): δ = 1.40–2.10 (m, 10H, C*H*$_2$); 2.82 (m, 2H); 3.02 (m, 2H); 3.23 (d, ^3J = 10.9 Hz, 1H); 3.35 (d, ^3J = 11.1 Hz, 1H); 3.45–3.60 (m, 2H); 3.63, 3.64, 3.72, 3.73 (s, 12H, –OC*H*$_3$); 3.99 (d, ^3J = 10.8 Hz, 2H); 4.10 (d, ^3J = 8.9 Hz, 2H); 4.65 (s, 2H, py–C*H*–N); 7.75–7.95 (m, 22H, H_{Ar}); 8.30–8.50 (m, 4H, H_{Ar}). ^{13}C NMR (50 MHz, $CDCl_3$): δ = 21.42, 25.94, 50.34, 52.20, 52.34, 53.68, 54.19, 54.61, 62.72, 63.46, 68.97, 71.87, 122.18, 122.98, 124.75, 125.10, 127.56, 128.32, 128.45, 136.09, 136.58, 140.89, 148.69, 149.40, 156.66, 169.74, 170.27. MS: FAB $C_{31}H_{32}N_4O_5$ $[M+H]^+$ = 541.4. $[\alpha]^D_{20}$ = 5.4° (S,rac) (c = 1 in $CHCl_3$).

3.2.5. (rac)-[(L^1)Cu(OTf)]OTf∗H_2O

L^1 (400 mg, 0.86 mmol) und Cu(OTf)$_2$ (312 mg, 0.86 mmol) in MeCN (water-free, 10 ml) were stirred under Ar for 6 h. The blue solution was reduced to approx. 5 ml (vacuum), and Et_2O (10 ml) was slowly diffused into this solution. The resulting blue solid was collected and crystallized from MeCN/Et_2O. Yield: 350 mg (0.4 mmol, 47%), blue solid. *Anal.* Calc. for $C_{27}H_{30}CuF_6N_4O_{12}S_2$: C, 38.41; H, 3.58; N, 6.64. Found: C, 38.27; H, 3.69; N, 6.72%. MS: FAB $C_{27}H_{30}CuF_6N_4O_{12}S_2$, $[(L^7)Cu(OTf)]^+$ = 677.1 (calc.: 677.1).

3.2.6. (R,rac)-[(L^2)Cu(OTf)]OTf∗H_2O∗MeOH

(R,rac)-L^2 (200 mg, 0.4 mmol) and Cu(OTf)$_2$ (137 mg, 0.4 mmol) in MeOH (water-free, 5 ml) were stirred under Ar at ambient temperature for 6 h. The blue solution was reduced to approx. 2 ml (vacuum), and Et_2O (5 ml) was slowly diffused into this solution. The resulting blue solid was collected and crystallized from MeOH/Et_2O. Yield: 170 mg (0.19 mmol, 48%), green solid. *Anal.* Calc. for $C_{29}H_{36}CuF_6N_4O_{13}S_2$: C, 39.12; H, 4.08; N, 6.29. Found: C, 39.54; H, 4.32; N, 6.36%. MS: FAB $C_{29}H_{36}CuF_6N_4O_{13}S_2$, $[(L^7)Cu(OTf)]^+$ = 691.2 (calc.: 691.2); $[(L^7)Cu(OTf)](H_2O)^+$ = 709.3 (calc.: 709.2); $[(L^7)Cu(OTf)](MeOH)^+$ = 723.2 (calc.: 723.2).

3.2.7. (S,rac)-[(L^3)Cu(OTf)]OTf∗H_2O∗MeOH

(S,rac)-L^3 (200 mg, 0.37 mmol) and Cu(OTf)$_2$ (127 mg, 0.37 mmol) in MeOH (water-free, 5 ml) were stirred under Ar at ambient temperature for 6 h. The blue solution was reduced to approx. 2 ml

(vacuum), and Et_2O (5 ml) was slowly diffused into this solution. The resulting blue solid was collected and crystallized from MeOH/Et_2O. Yield: 144 mg (0.15 mmol, 40%), blue solid. *Anal.* Calc. for $C_{34}H_{38}CuF_6N_4O_{13}S_2$: C, 42.88; H, 4.02; N, 5.88. Found: C, 42.68; H, 4.14; N, 5.90%. MS: FAB $C_{29}H_{36}CuF_6N_4O_{13}S_2$, $[(L^9)Cu(OTf)]^+$ = 753.2 (calc.: 753.2); $[(L^9)Cu(OTf)](H_2O)^+$ = 771.2 (calc.: 771.2); $[(L^9)Cu(OTf)](MeOH)^+$ = 785.3 (calc.: 785.3).

3.2.8. (R,R)-[(L^2)Cu(OH_2)](BF_4)$_2$/(R,S)-[(L^2)Cu(OH_2)](BF_4)$_2$

(R,rac)-L^2 (200 mg, 0.4 mmol) and $Cu(OTf)_2$ (137 mg, 0.4 mmol) in MeOH (water-free, 10 ml) were stirred under Ar at ambient temperature for 6 h. The blue solution was added to H_2O (500 ml) and sorbed onto a ion exchange column (Sephadex CM25, 200 eq, 80 g). The complex was eluted with sodium (L)-tartrate (0.1 M) until two fully separated bands were visible. The column was then washed with H_2O (1500 ml), and the two isomers were then eluted with $NaBF_4$. These solutions were reduced in volume on a rotavap, and the $NaBF_4$ salt was reduced by addition of EtOH/cooling/filtration. The solids (1st band: R,S-, 2nd band: R,R-isomer) were then crystallized from MeOH/Et_2O. Single crystals for an X-ray crystal structure analysis were obtained from the 1st fraction, eluted with 0.1 M NaCl (chloro complex). $[\alpha]^{632.5}_{20} = -53.3^\circ$ (R,S) (c = 1 in $CHCl_3$), $[\alpha]^{632.5}_{20} = 1.9^\circ$ (R,R) (c = 1 in $CHCl_3$). *Anal.* Calc. for $C_{26}H_{32}B_2CuF_8N_4O_6$: C, 42.56; H, 4.40; N, 7.64. Found: C, 42.86; H, 4.39; N, 7.62%.

3.3. X-ray crystal structure determinations

Crystal data and details of the structure determinations are listed in the Supplementary material (Table S1). Intensity data were collected at low temperature (100(2) K) with a Bruker AXS Smart 1000 CCD diffractometer (Mo Kα radiation, graphite monochromator, λ = 0.71073 Å). Data were corrected for air and detector absorption, Lorentz and polarization effects [36]; absorption by the crystal was treated with a semi-empirical multiscan method [37,38]. The structures were solved by conventional direct methods (L^1, L^2 and [L^2)Cu(Cl)]Cl) [39,40] or by the charge flip procedure (L^3) [41,42] and refined by full-matrix least squares methods based on F^2 against all unique reflections [40,43]. All non-hydrogen atoms were given anisotropic displacement parameters. Hydrogen atoms were generally input at calculated positions and refined with a riding model. When justified by the quality of the data the positions of some hydrogen atoms were taken from difference Fourier syntheses and refined. Similarity restraints were applied during refinement of L^2. Some pyridyl rings of the free ligands L^1 (py2) and L^3 (py1) were found disordered and were refined with split-atom models.

3.4. Computational details

Geometry optimizations of all four diastereomers were carried out using GAUSSIAN 03 [44]. The B3LYP hybrid functional was used in combination with a triple-ζ 6-311G* basis on Cu and all heavy atoms and 6-31G basis on all hydrogens [44–46] (B1). The optimizations were carried out with no constraints and the structures were verified for minima by performing frequency calculations using the same method. In addition, the effect of solvent and a larger basis (6-311+G**) were accounted (B2). The self-consistent reaction field (COSMO) as implemented in G03 was used by inputting acetonitrile as the solvent. There were no significant changes on inclusion of the solvent and the larger basis and hence the relative energies reported in the paper are at the B3LYP/B1 level unless otherwise stated. All LFMM calculations were carried out using DOMMIMOE [26], an extended version of Molecular Operating Environment [47]. The MMFF94_TM force field that was previously shown to perform well for Cu–bispidine complexes was used in the present study [12]. The angular overlap model (AOM) calculations were carried out using CAMMAG, a ligand field program [48]. The electronic parameters (e_σ, e_{ds}, spin–orbit coupling) used in the AOM calculations were similar to those described previously (see Supplementary information for the ligand field parameters) [32,49–52].

Acknowledgment

Generous financial support by the German Science Foundation (DFG) is gratefully acknowledged.

Appendix A. Supplementary material

CCDC 809607–809610 contain the supplementary crystallographic data for this paper. These data can be obtained free of charge from The Cambridge Crystallographic Data Centre via www.ccdc.cam.ac.uk/data_request/cif. Supplementary data associated with this article can be found, in the online version, at doi:10.1016/j.ica.2011.02.047.

References

[1] H. Börzel, P. Comba, C. Katsichtis, W. Kiefer, A. Lienke, V. Nagel, H. Pritzkow, Chem. Eur. J. 5 (1999) 1716.
[2] H. Börzel, P. Comba, K.S. Hagen, C. Katsichtis, H. Pritzkow, Chem. Eur. J. 6 (2000) 914.
[3] H. Börzel, P. Comba, H. Pritzkow, J. Chem. Soc., Chem. Commun. (2001) 97.
[4] H. Börzel, P. Comba, K.S. Hagen, M. Kerscher, H. Pritzkow, M. Schatz, S. Schindler, O. Walter, Inorg. Chem. 41 (2002) 5440.
[5] P. Comba, M. Merz, H. Pritzkow, Eur. J. Inorg. Chem. (2003) 1711.
[6] K. Born, P. Comba, R. Ferrari, S. Kuwata, G.A. Lawrance, H. Wadepohl, Inorg. Chem. 46 (2007) 458.
[7] P. Comba, M. Kerscher, W. Schiek, Prog. Inorg. Chem. 55 (2007) 613.
[8] P. Comba, A. Lienke, Inorg. Chem. 40 (2001) 5206.
[9] P. Comba, A. Hauser, M. Kerscher, H. Pritzkow, Angew. Chem., Int. Ed. 42 (2003) 4536.
[10] P. Comba, C. Lopez de Laorden, H. Pritzkow, Helv. Chim. Acta 88 (2005) 647.
[11] P. Comba, B. Martin, A. Prikhod'ko, H. Pritzkow, H. Rohwer, C. R. Chim. 6 (2005) 1506.
[12] A. Bentz, P. Comba, R.J. Deeth, M. Kerscher, H. Pritzkow, B. Seibold, H. Wadepohl, Inorg. Chem. 47 (2008) 9518.
[13] P. Comba, M. Kerscher, M. Merz, V. Müller, H. Pritzkow, R. Remenyi, W. Schiek, Y. Xiong, Chem. Eur. J. 8 (2002) 5750.
[14] P. Comba, W. Schiek, Coord. Chem. Rev. 238–239 (2003) 21.
[15] P. Comba, C. Haaf, H. Wadepohl, Inorg. Chem. 48 (2009) 6604.
[16] W.-D. Stohrer, R. Hoffmann, J. Am. Chem. Soc. 74 (1972) 779.
[17] G. Parkin, Chem. Rev. 93 (1993) 887.
[18] G. Parkin, R. Hoffmann, Angew. Chem. 106 (1994) 1530.
[19] M.M. Rohmer, M. Bénard, Chem. Soc. Rev. 30 (2001) 340.
[20] C.L. Exstrom, D. Britton, K.R. Mann, G. Hill, V.M. Miskowski, W.P. Schaefer, H.B. Gray, W.M. Lamanna, Inorg. Chem. 35 (1996) 549.
[21] K. Born, P. Comba, M. Kerscher, H. Rohwer, Dalton (2009) 362.
[22] P. Comba, M. Kerscher, Coord. Chem. Rev. 253 (2009) 564.
[23] F. Lions, A.M. Willison, J. Proc. R. Soc. New South Wales 73 (1940) 240.
[24] A.W. Addison, T.N. Rao, J. Reedijk, J. van Rijn, G. Verschoor, J. Chem. Soc., Dalton Trans. (1984) 1349.
[25] V.J. Burton, R.J. Deeth, C.M. Kemp, P.J. Gilbert, J. Am. Chem. Soc. 117 (1995) 8407.
[26] R.J. Deeth, N. Fey, B.J. Williams-Hubbard, J. Comp. Chem. 26 (2005) 123.
[27] P. Comba, R. Remenyi, Coord. Chem. Rev. 238–239 (2003) 9.
[28] P. Comba, V. Müller, R. Remenyi, J. Inorg. Biochem. 98 (2004) 896.
[29] M. van Gastel, G.W. Canters, H. Krupka, A. Messerschmidt, E.C. de Waal, G.C.M. Warmerdam, E.J.J. Groenen, J. Am. Chem. Soc. 122 (2000) 2322.
[30] M. Gerloch, Magnetism and Ligand-Field Analysis, Cambridge University Press, 1983.
[31] H. Stratemeier, M.A. Hitchman, P. Comba, P.V. Bernhardt, M.J. Riley, Inorg. Chem. 30 (1991) 4088.
[32] P. Comba, T.W. Hambley, M.A. Hitchman, H. Stratemeier, Inorg. Chem. 34 (1995) 3903.
[33] P. Comba, Coord. Chem. Rev. 182 (1999) 343.
[34] M. Atanasov, P. Comba, B. Martin, V. Müller, G. Rajaraman, H. Rohwer, S. Wunderlich, J. Comp. Chem. 27 (2006) 1263.
[35] G.R. Hanson, K.E. Gates, C.J. Noble, M. Griffin, A. Mitchell, S. Benson, J. Inorg. Biochem. 98 (2004) 903.
[36] G.M. Sheldrick, SADABS, Bruker AXS Madison, 2004–2008.
[37] R.H. Blessing, Acta Crystallogr., Sect. A 51 (1995) 33.
[38] G.M. Sheldrick, SADABS-2004, first ed., Bruker AXS, Madison, Wisconsin, Göttingen, 2004–2008.

[39] G.M. Sheldrick, SHELXS, Program for Structure Solution, 97 ed., University of Göttingen, Göttingen, 1997.
[40] G.M. Sheldrick, Acta Crystallogr., Sect. A 64 (2008) 112.
[41] L. Palatinus, SUPERFLIP, EPF Lausanne, Switzerland, 2007.
[42] L. Palatinus, G. Chapuis, J. Appl. Crystallogr. 40 (2007) 789.
[43] G.M. Sheldrick, SHELXL-97, University of Göttingen, Göttingen, 1997.
[44] M.J. Frisch, G.W. Trucks, H.B. Schlegel, G.E. Scuseria, M.A. Robb, J.R. Cheeseman, J.A. Montgomery Jr., T. Vreven, K.N. Kudin, J.C. Burant, J.M. Millam, S.S. Iyengar, J. Tomasi, V. Barone, B. Mennucci, M. Cossi, G. Scalmani, N. Rega, G.A. Petersson, H. Nakatsuji, M. Hada, M. Ehara, K. Toyota, R. Fukuda, J. Hasegawa, M. Ishida, T. Nakajima, Y. Honda, O. Kitao, H. Nakai, M. Klene, X. Li, J.E. Knox, H.P. Hratchian, J.B. Cross, V. Bakken, C. Adamo, J. Jaramillo, R. Gomperts, R.E. Stratmann, O. Yazyev, A. Austin, R. Cammi, C. Pomelli, J.W. Ochterski, P.Y. Ayala, K. Morokuma, G.A. Voth, P. Salvador, J.J. Dannenberg, V.G. Zakrzewski, S. Dapprich, A.D. Daniels, M.C. Strain, O. Farkas, D.K. Malick, A.D. Rabuck, K. Raghavachari, J.B. Foresman, J.V. Ortiz, Q. Cui, A.G. Baboul, S. Clifford, J. Cioslowski, B.B. Stefanov, G. Liu, A. Liashenko, P. Piskorz, I. Komaromi, R.L. Martin, D.J. Fox, T. Keith, M.A. Al-Laham, C.Y. Peng, A. Nanayakkara, M. Challacombe, P.M.W. Gill, B. Johnson, W. Chen, M.W. Wong, C. Gonzalez, J.A. Pople, GAUSSIAN Inc., Wallingford, CT, 2004.
[45] A.D. Becke, J. Chem. Phys. B 98 (1993) 5648.
[46] C. Lee, W. Yang, R.G. Parr, Phys. Rev. B 37 (1988) 785.
[47] Chemical Computing Group, 2007.09 ed., Montreal, 2007.
[48] D.A. Cruse, J.E. Davies, M. Gerloch, J.H. Harding, D.J. Mackey, R.F. McMeeking, CAMMAG, A Fortran Program for AOM Calculations, University Press Cambridge, Cambridge, 1980.
[49] P. Comba, P. Hilfenhaus, B. Nuber, Helv. Chim. Acta 80 (1997) 1831.
[50] P. Comba, H. Pritzkow, W. Schiek, Angew. Chem. 113 (2001) 2556.
[51] P. Comba, in: J.K.A. Howard, F.H. Allen, G.P. Shields (Eds.), Implications of Molecular and Materials Structure for New Technologies, Kluwer, Dordrecht, 1999, p. 87.
[52] R.G. McDonald, M.J. Riley, M.A. Hitchman, Inorg. Chem. 27 (1988) 894.